Precision Engineering 48 (2017) 331–337

Contents lists available at ScienceDirect

Precision Engineering

journal homepage: www.elsevier.com/locate/precision

Visualization of fluctuations in internal stress distribution of workpiece during ultrasonic vibration-assisted cutting

Hiromi Isobe [a,*], Keisuke Hara [b]

[a] Nagaoka University of Technology, Department of Mechanical Engineering, Kamitomioka 1603-1, Nagaoka, Niigata 942-2188, Japan
[b] National Institute of Technology, Ichinoseki College, Department of Mechanical Engineering, Takanashi, Hagisho, Ichinoseki, Iwate, Japan

ARTICLE INFO

Article history:
Received 27 December 2016
Accepted 3 January 2017
Available online 10 January 2017

Keywords:
Ultrasonic vibration cutting
Photoelastic method
Stress distribution
Orthogonal cutting
Stroboscopic effect

ABSTRACT

The aim of this study is to construct visualization system of stress distribution under ultrasonic vibration-assisted cutting condition in order to investigate the cutting phenomenon. The vibrating cutting edge is considered to be cause of dynamic change of cutting force at ultrasonic frequency. However, many researchers have explained the effect of ultrasonic vibration-assisted cutting by evaluating the time-averaged cutting force, because it is difficult to measure the dynamic cutting force by using dynamometers. In this study, the instantaneous stress distribution on workpiece was visualized by photoelastic method in combination of pulse laser emission synchronized with vibration of cutting edge. Orthogonal cutting test was carried out at low cutting speed relative to vibration speed of insert. A constructed photographic system divided the ultrasonic vibration period of 36.2 μs into 360 points and took one photograph frame at each point. By counting the number of criteria pixels which images the cutting stress, the intermittent cutting condition was evaluated. It was experimentally confirmed that the stress distribution under vibration-assisted condition showed the periodical change synchronized with insert vibration. Because these results are compatible with well-known vibration cutting theories, the imaging system is able to show the periodic change of stress distribution in ultrasonic frequency band. The intermittent cutting condition was affected not only feed speed but also depth of cut. The theory of relative motion between tool and workpiece is insufficient to explain these results. Therefore, remnants formed due to elastic deformation of the workpiece were examined. The vibration cutting dramatically reduced the elastic deformation and the vibration amplitude had effect on the amount of remnant thickness.

1. Introduction

Carbon fiber reinforced plastics (CFRPs) and other resin-based composite materials are used in fields from aeronautical components to automotive components. Consequently, there is a demand for methods for removing burrs from thermoplastic resins quickly and highly accurately. Ultrasonic vibration-assisted cutting, in which the cutting edge of tool is vibrated in the ultrasonic range of frequencies, is employed for lathe turning of heat-resistant alloys [1–4]. Ultrasonic drilling of titanium-alloys [5,6] experimentally shown to suppress tool wear and reduce cutting resistance. High-speed camera captured the vibration mode of small diameter drill. Experimentally demonstrated that longitudinal vibration mode provided the chisel edge to bite the workpiece, which eliminate the tool wear due to the slip, in contrast to bending vibration mode accelerated tool wear. Wang et al. [7] showed the ultrasonic drilling to be helpful for the machining of holes on quartz glass. The machining-induced crack was reproduced by carefully applied static force to demonstrate the formation of edge chipping. Unique approach for smaller diameter drilling was reported [8]. A sintered carbide grinding wheel formed by WEDM was vibrated in axial direction. The helical feed tool path with rotation drilled micro-holes 30, 20 and 10 μm in diameter. The assistance of ultrasonic vibration reduced grinding force by reduction of chip clogging and friction. Lv et al. [9] investigated the groove surface formation of glass by rotary ultrasonic machining. Loci of diamond grains were considered and scratches are carefully investigated by white-light interferometer and SEM. The specimen surface showed the effect of fluctuation of abrasive inertia and periodic variation in effective workpiece angle. Elliptical vibration cutting [10,11] has excellent performance to achieve ultraprecision machining of difficult-to-cut material. The tool motion pulls up the chip upward. The pulling

* Corresponding author.
E-mail addresses: isobe163@mech.nagaokaut.ac.jp (H. Isobe), hara@ichinoseki.ac.jp (K. Hara).

http://dx.doi.org/10.1016/j.precisioneng.2017.01.003
0141-6359/

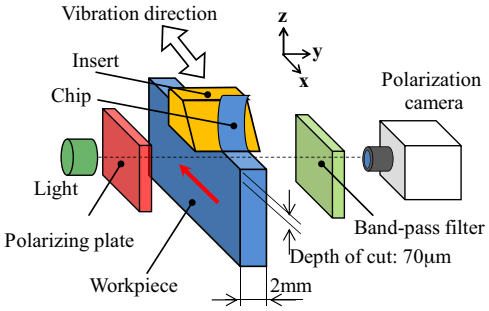

Fig. 1. Configuration of photoelastic experiment.

force decreases friction between tool and chip and reduces chip thickness and cutting force.

It is fundamentally difficult to take direct measurements of the events occurring during the formation of chips by tools vibrating in the ultrasonic range and to prove such characteristics theoretically. In our current research, we observed orthogonal cutting of methacrylate resin by a photoelastic method, calculated the cutting force from the fringe order for comparison with the cutting force measured by a tool dynamometer, and found a method for estimating the cutting force [12]. By pulsing an LED light source at 3.6 μs, which corresponds to 1/12 of a period of the ultrasonic vibration of the cutting edge of tool, we photographed the fluctuating stress distribution in the vibrating cutting edge. In the intermittent cutting condition during ultrasonic vibration-assisted cutting, periods were found when the cutting stress disappeared completely.

For this study, a system was assembled with a pulsed laser to examine the short-period fluctuations in stress. We also examined whether fluctuations in the stress distribution due to vibration of the tool were affected by the vibration amplitude or the feed speed. Other phenomena of ultrasonic cutting were observed as well, including the remnants left due to elastic deformation of the workpiece.

2. Experimental method

2.1. Imaging of stress distribution by the photoelastic method

It is well known that clear, uniform materials exhibit birefringence when subjected to a stress from an exterior force. Employing birefringence to examine the stress conditions inside an object is called the "photoelastic method." In our experiment, the stress distribution in a workpiece was observed by the photoelastic method during the cutting process. A light source, a circular polarizer, a band pass filter, and a polarization camera [13] were placed as shown in Fig. 1 to make high-speed observations of the cutting point and the distribution of birefringence. This system, categorized as a semicircular polarizer used in transmission photoelasticity [14], provides information about the phase difference between the directions of maximum principal stress and minimum principal stress. As a result of birefringence, the phase difference of the light beams is then proportional to the difference between the principal stresses, as long as the deformation remains within the elastic zone. When the workpiece is assumed to be an elastic body and is only subject to a uniform line load in the thickness direction due to cutting force, Flamant [15] showed that the stress distribution arising in the workpiece adjacent to the tip of the insert is a simple circular stress distribution. Thus, the internal stress distribution of the workpiece is a simple stress condition. Our previous paper [12] demonstrated that cutting forces can be calculated from the observed principal stress distribution

2.2. Photography by stroboscopic effect

A camera used to film the stress fluctuations accompanying low-amplitude ultrasonic vibrations must have sufficient pixels to accommodate a high frame rate and spatial resolution. It is incompatible for even a high-speed camera to fulfill both requirements. Therefore, for this study, a pulsed laser with a pulse duration much shorter than the vibration period was set to match the vibration frequency of the tool that it illuminated. The light source was a Q-switched ND:YVO4 laser; its specifications stated that it had a pulse duration of 15 ns with a timing stability of 3% (σ). Fig. 2 shows the timing of the camera trigger, exposure, insert vibration and the laser irradiation trigger, which was matched to the insert vibration. In this study, the frame rate of the high-speed camera was 6000 fps, the frame size was 896 × 752 pixels, and the shutter open time was 1/25000 s. When exposure was started with arbitrary timing by the camera start trigger, a camera sync out signal was output from the camera at every frame. However, in the bolt-clamped Langevin type ultrasonic transducer, which was the ultrasonic actuator, an alternating voltage was applied by the oscillation power supply in response to the 36.2 μs-period excitation signal. When it detected the down signal of the excitation signal after detecting the down edge of the camera sync out signal, it transmitted a laser irradiation signal to the laser oscillator after a delay of 0.1 μs multiplied by frame number *N*. After the laser irradiation signal was triggered, the laser was activated to illuminate the cutting point after a fixed time of 0.35 μs. The laser then illuminated the cutting point in-phase of the ultrasonic vibration for 15 ns. Then, while the shutter was opened for one period of ultrasonic vibration, the camera was exposed to a single "shot" by the laser illumination. From the second frame on, the exposures were successively delayed with respect to the phase of the ultrasonic vibration by 0.1 μs, so that after a total of 362 exposures, one complete period of ultrasonic vibration was recorded.

2.3. Cutting setup

In this experiment, two-dimensional cutting was employed as it is a simple case allowing a comparative investigation between the cutting force vectors according to the stress distribution and the theory of cutting phenomena. When the workpiece feed is in the same direction as the vibratory motion, this is principal direction ultrasonic cutting. Thus, an intermittent cutting condition in which the workpiece and cutting edge of tool separate from each other is established by their relative motion. The vibrating cutter unit consists of the insert attached to the tip of the horn and it is vibrated by a bolt-clamped Langevin type ultrasonic transducer. The longitudinal vibratory mode of the horn was designed and manufactured to match the resonant frequency of 27.8 kHz. The uncoated cemented carbide insert had a rake angle of 10° and a clearance angle of 7°. The polarization camera and ultrasonic cutting unit were clamped in their positions in order to fix the area for taking photographs of the cutting point and to make regular observations while the workpiece was fed into the camera field of view. Therefore, tool oscillations and fluctuations in stress distribution could be observed in the stationary coordinate system of the camera. The vibration amplitude of the insert was set by adjusting the amplitude of the alternating voltage applied to the transducer.

For the methacrylate resin workpiece, we used cast material, which has greater isotropy and uniformity in its mechanical and optical properties than does extruded methacrylate. The cut thickness (workpiece thickness) was 2 mm and the workpiece was fed at a uniform speed by the feed mechanism.

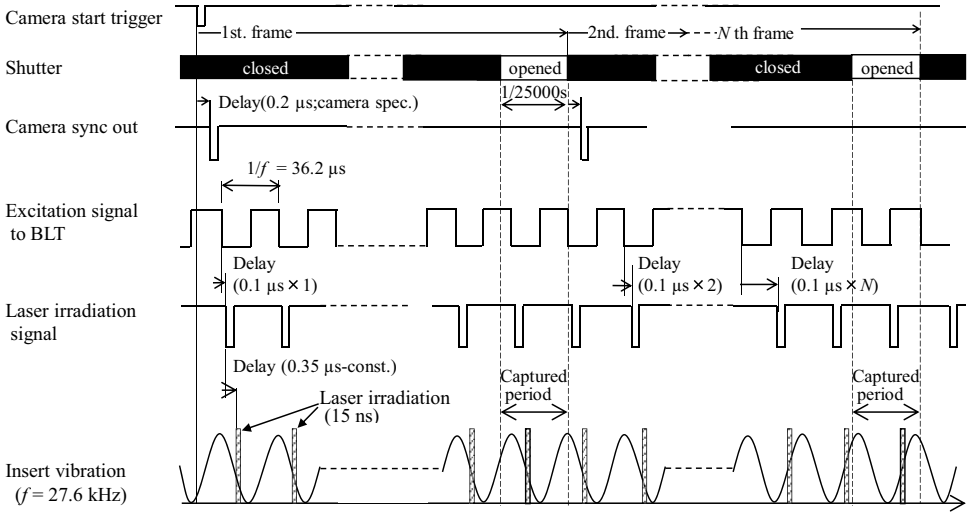

Fig. 2. Timing chart.

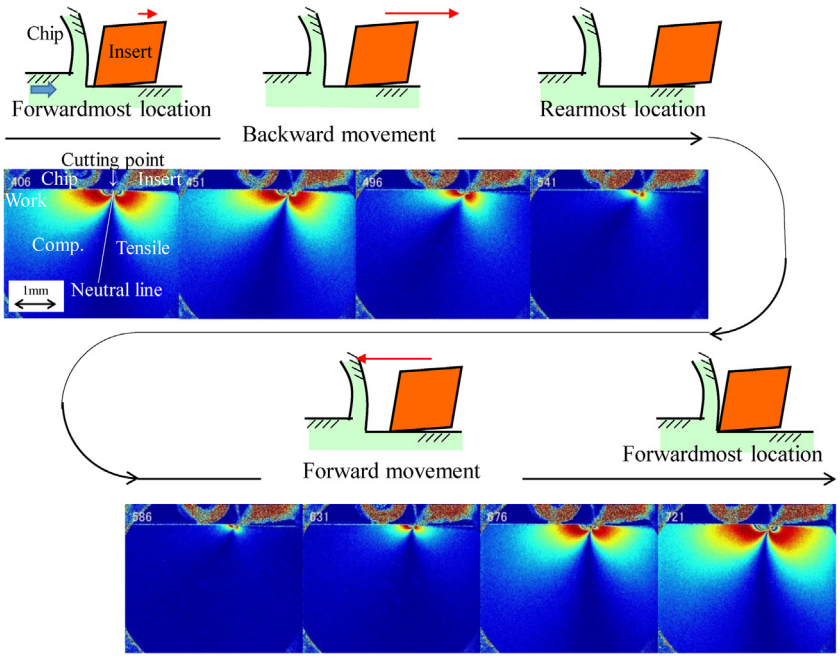

Fig. 3. Variation of stress distribution for one period of ultrasonic vibration of tool.

3. Experimental results

3.1. Time-varying stress distribution in ultrasonic frequency

The time-varying stress distribution for one period of ultrasonic vibration of 36.2 μs with depth of cut of 30 μm is shown in Fig. 3. As explained in Section 2.1, the one shot of stress distribution is captured by emission of pulse laser for 15 ns radiation. The series of photos represents the change of stress distribution for a cycle of tool vibration when the tool is in most advanced location, moved backward, in backward location and moved forward. When tool is cutting workpiece, the cutting force results in stress widely spread below cutting point. Narrower fringe distance means the intensive stress. The neutral line is drawn from cutting point through zero principal stress. Typical stress distribution under orthogonal cutting: the compression and tensile stress spread across the neutral line. The principal stress of 0 and 15 MPa is valued as blue and red, respectively. The calibration method is described in following section.

3.2. Method for assessing stress distribution

Pictures of the phase difference were taken with the constructed photography system. The phase difference is proportional to the principal stress magnitude in the 2-dimensional cutting condition. As an example, Fig. 4(a) shows the frame at the instant when the stress reached its widest extent. The variation in phase difference accompanying the increase in stress is expressed as continuous hue changes, i.e., 0 (blue) → π/2 (red) → π (blue) → 3π/2 (red). The first fringe (red) corresponds to 15 MPa and the second fringe (red) corresponds to 30 MPa. However, the third and higher fringes are not visible. When an LED is employed as the light source [12], we can see as high as the fourth fringe, which is close to the yield stress of 75 MPa for methacrylate resin. Thus, the spatial resolution here may well have been degraded by speckle noise due to the laser

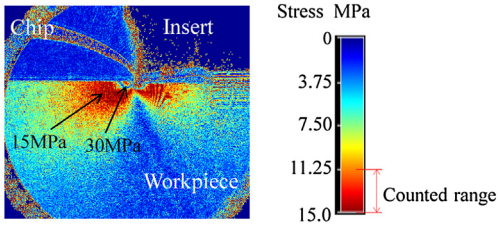

(a) Relationship between phase difference and stress

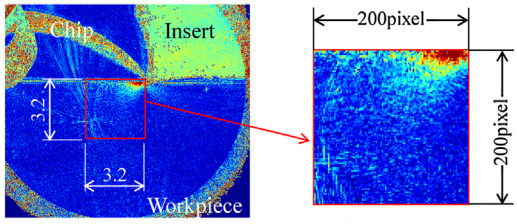

(b) Stress evaluation for 1st. fringe

Fig. 4. Instantaneous phase difference map. (For interpretation of the references to color in the text, the reader is referred to the web version of this article.)

source. Measures against this degradation must be taken in future examinations of the conditions near the cutting point. Nonetheless, it was possible to photograph the spread of the stress distribution in one shot with the laser illumination time of 15 ns, and this was verified to provide enough light intensity.

It is possible to geometrically calculate the magnitude and orientation of the cutting force from the observed principal stress distribution, if we assume a simple circular stress distribution. It is reported that the cutting forces are evaluated in a maximum stress distribution, where the stress distribution had spread widely and the third and fourth fringes were clearly visible [12]. However, there were narrow ranges where the tool and workpiece had just come into contact or had just separated and the stress field ranges were quite limited. Because it was not possible to plot the iso-stress circle geometrically, fluctuations in the cutting forces could not be assessed. Therefore, a region measuring 3.2 mm × 3.2 mm (200 × 200 pixels) was selected for observation as shown in Fig. 4(b). The numbers of pixels in the range of stresses showing high linearity of the operating stress-phase difference relation around the first fringe, i.e., from 11.25 MPa (orange) to 15.0 MPa (red), are here called "numbers of criteria pixels" (NCP) throughout this paper. Changes in the NCP with time are considered to be changes in the stress distribution.

3.3. Relationship between tool vibration and fluctuations in stress distribution

It is common to explain the vibration cutting phenomenon by relative speed between vibrating tool and workpiece which is approaches to tool with constant feed speed [16]. Here, the location of the vibrating tool is $x_c = a_0 \sin 2\pi ft$ and the speed of the workpiece approaching the tool is F (generally, a constant) as shown in Fig. 5. If the speed of the tool which moves in backward is greater than the workpiece feed speed, interrupted cutting occurs, and the rake face of the tool separates from the uncut material and the chip. The vibration frequency f was 27.6 kHz and the vibration amplitude a_0 was 6 μm. To elucidate the effectiveness of ultrasonic vibrations, the workpiece feed rate was set at F = 1.0 m/min, which was sufficiently lower than the instantaneous maximum speed of vibrating tool of 64.7 m/min. Thus, the cutting condition was interrupted cutting, in which theoretically the ultrasonically vibrating tool was repeated as intervals of contact and no contact with the workpiece. Fig. 6 shows the variation in the vibration speed of the tool near the

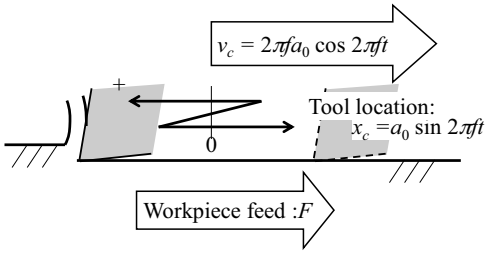

Fig. 5. Relative motion of tool and work.

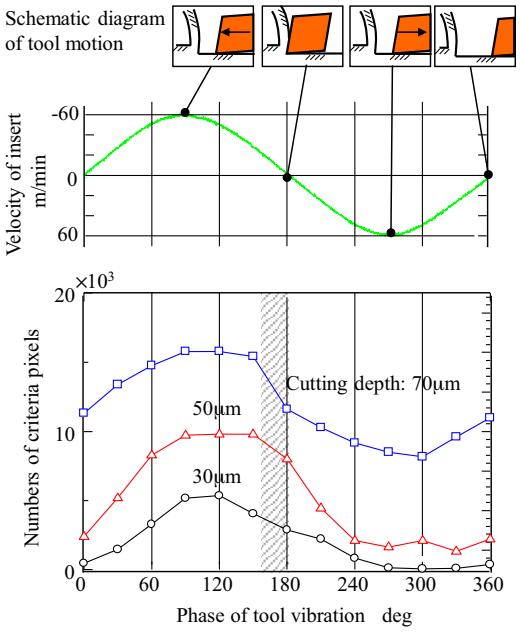

Fig. 6. Time varying stress distribution: a_0 = 6 μm, F = 1.0 m/min.

cutting point, measured by laser Doppler vibrometry (LDV) and the variation in the NCP. The depths of cut were 30, 50 and 70 μm. The base points for the tool vibration speed were the tool phase positions of the rearmost location (0°) and the forwardmost location (180°). From the rearmost location, the tool began with a speed of zero and approached the chip. The NCP also broadened and showed some phase lag with respect to the vibration speed. After the tool reached the neutral position of vibration, where the speed reached the maximum, the NCP reached its maximum size at a phase lag of about 45°. In other words, when the cutting was theoretically in the intermittent condition, it was found that the internal stress of the workpiece was in phase with the fluctuations in vibration velocity. In addition, as the tool went through its return stroke, the NCP shrank, but when the depth of cut was 70 μm, the NCP began to broaden before the tool reached the rearmost location. That is, the NCP size never "flattened" at a low value. In contrast, when the depth of cut was 30 or 50 μm, after the phase angle of 240°, the NCP remained small until phase angle 330°. Tensile stresses, probably due to abrasion between the clearance face and surface to be machined, were also factors adding to the stress, so the NCP never fell to zero. This suggests that there was a period when the tool was out of physical contact with the chip and uncut workpiece. In other words, even when the feed speed was lower than the critical rate, a large depth of cut caused a transition from the intermittent cutting condition to the continuous cutting condition.

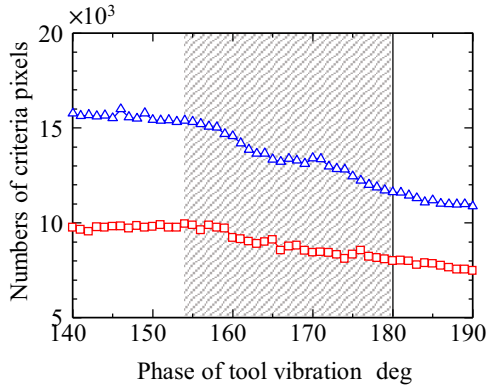

Fig. 7. Magnified graph for theoretical contact period.

3.4. Stress fluctuations just after contact

Let us consider the relative motion between the ultrasonic vibration of the tool and the feed motion of the workpiece. During intermittent cutting, at the instant of contact between the tool and the workpiece, the tool collides with the workpiece at a certain velocity due to its vibration, and this can be expected to cause an impulsive fluctuation in the stress due to the collision energy resulting from the tool striking the workpiece. In this experiment, the contact time between the tool and workpiece, derived from their relative motion, is estimated at 2.6 μs. One cycle at the ultrasonic frequency is 36.2 μs, so the contact period corresponds to the phase angle at the ultrasonic frequency of 26°. Hash marks were added to Fig. 6 to represent the theoretical contact period of 26°. Fig. 7 presents the magnified graph for theoretical contact period with sampling intervals of 0.1 μs. The propagation speed of the longitudinal elastic waves in the methacrylate resin is 2730 m/s. This corresponds to 0.27 mm of travel during one sampling interval. It was possible for the present photography system to photograph the propagation behavior of an elastic wave within the camera field of view, but it was not possible to witness impulsive changes. Thus, it was found that the machining phenomena in the context of intermittent cutting theory cannot be explained only by the relative displacements of the tool and workpiece.

3.5. Variation in effectiveness of ultrasonic vibrations with cutting conditions

Let us next examine the influence of machining conditions on the effectiveness of ultrasonic vibration cutting by demonstrating the changes in the NCP with time when the feed speed and vibration amplitude are set to half the values employed in the previous section. Fig. 8(a) shows that when the feed speed is reduced from 1.0 m/min to 0.5 m/min, the ultrasonic vibration speed becomes a higher multiple of the feed speed. As a result, the fluctuation curve representing the NCP diminishes at all depth of cuts. Specifically, at depth 30 μm and feed speed 1.0 m/min (Fig. 6(a)), the NCP shrinks during the 270°–360° phase, while at a feed speed of 0.5 m/min, the region remains small for over half a complete cycle. The time of contact between the tool and the uncut workpiece is relatively shortened, and the period where reaction stress disappeared is extended. Fig. 8(b) shows the results when the vibration amplitude was reduced from 6 μm to 3 μm. The dashed lines in the figure show the NCP when non-vibration cutting, or, in other words, steady-state NCP when the vibration amplitude was reduced to 0 μm. This indicates that the instantaneous maximum cutting force during ultrasonic vibration was approximately equal to that of non-vibration. Thus, increasing the amplitude of ultrasonic vibration

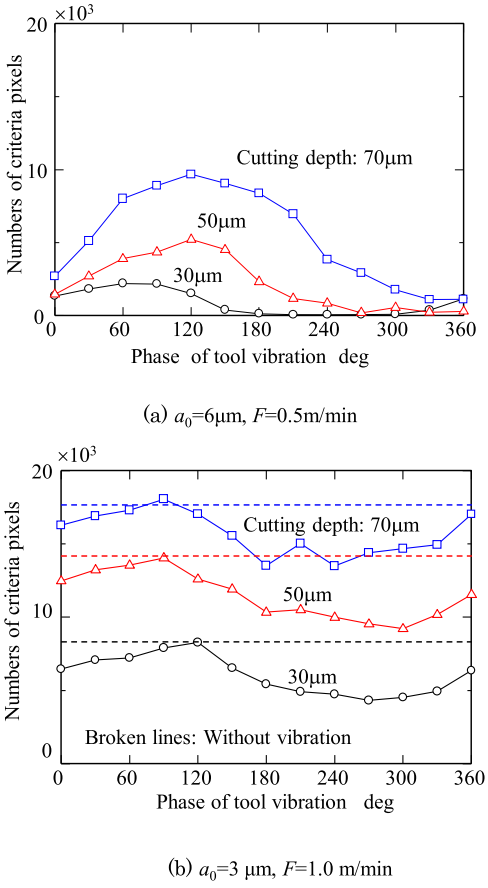

Fig. 8. Effect of cutting parameters on stress distribution.

moderate the stress level at a certain phase of the vibratory period, not throughout the vibratory period.

3.6. Measurement of uncut remnant thickness due to elastic recovery

So far in this experiment, in spite of the fact that the tool was theoretically in the intermittent cutting condition due to ultrasonic vibration, it was not possible to verify this from the fluctuations in stress distribution. One of the reasons for this could be the presence of remnants due to elastic recovery of the workpiece. Fig. 9(a) shows the coordinate system used for measuring remnants, where a_0 is the tool oscillation amplitude in ultrasonic vibration machining. The center of vibration is defined as the origin of tool position x_{tool} for measuring the uncut remnant thickness. The position of the tool measured by a laser displacement sensor after stopping the vibration revealed that it stopped on the midpoint of the oscillation, where is the origin of x_{tool}. The experiment was initiated 2 min after the sudden stop of workpiece feed had been activated during cutting to verify that no changes in the stress distribution had occurred and to avoid any influence on the stress from the heat of cutting. If the tool causes only plastic deformation from $x_{tool} = +a_0$ to $-a_0$, there is no remaining uncut. In other word, no cutting force occurs where the tool is any position from $+a_0$ to $-a_0$. In actual cutting, elastic recovery of workpiece and/or chip results in remaining uncut d_e as shown in Fig. 9(b). When the tool position x_{tool} is less than $d_e - a_0$, the tool pushes back the chip and the acting force is increased. By measuring the acting force, the amount of remaining uncut with/without ultrasonic vibrating tool. Fig. 9(c) shows the tool force (acting force) acting on the workpiece as it varied with tool position. At the depth of cut of 50 μm, the

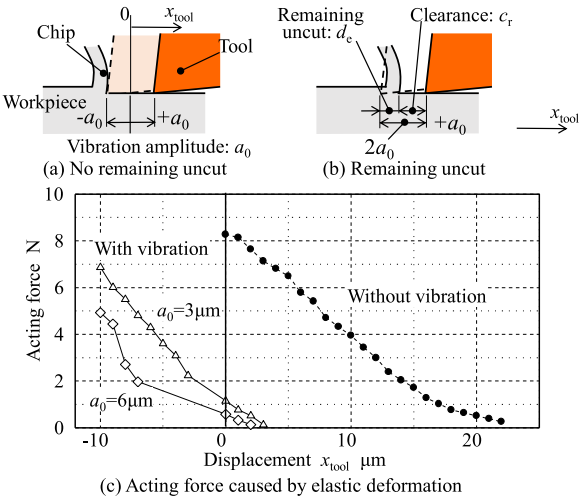

Fig. 9. Decrease of remaining uncut by vibration.

tool was advanced in very small increments at the extremely slow workpiece feed speed of 0.1 m/min. The horizontal axis represents the tool position, and the negative values here mean that the tool was stopped and then forced farther into the workpiece. The acting force was calculated in the same way as in our previous report, by using a phase difference map and the photography method with an LED light source, which is only slightly affected by speckle noise caused by coherence of laser. The acting force after stopping the feed was 8.2 N when the vibration was not activated. The acting force subsided while the tool was being withdrawn, and nearly disappeared once the tool had been withdrawn more than 22 μm. In other word, remaining uncut is estimated to be 22 μm without vibration condition. During vibration cutting, just after stopping the feed, the acting force was 1.2 N at the vibration amplitude of 3 μm and 0.6 N at the vibration amplitude of 6 μm. If we assume that there are no remnants during vibration cutting, we can consider the acting force to be zero when the tool is inserted until $x_{tool} = -a_0$. However, the acting force that actually existed after the vibration was stopped increased in approximate proportion with the displacement during the tool insertion, so it is reasonable to assume that the tool was in contact with the uncut face of the workpiece when the vibration was stopped. When the vibration amplitude was 3 μm, the acting force fell to zero at $x_{tool} = 3$ μm. In ultrasonic cutting condition, then, the tool was in constant contact with the uncut portion of the workpiece, so this was not the intermittent cutting condition. The condition, at which the acting force dropped to zero when the vibration amplitude was 6 μm and the tool had been withdrawn just 2 μm, can be considered intermittent cutting. In the previous section, it was noted that the NCP never shrank to zero at any time during the ultrasonic vibratory cycle when feed speed was sufficiently smaller than critical cutting speed at the vibration amplitude of 3 μm. From these results, it is confirmed to attribute the non- intermittent cutting to the elastic deformation of the workpiece. In order to realize intermittent cutting condition, not only the feed speed is less than critical cutting speed calculated theoretically by relative motion between tool and workpiece, but also the sufficient vibration amplitude is required to reduce the amount of uncut remnant than amplitude.

4. Conclusion

The photoelastic method and strobe photography were combined to take measurements of the fluctuations in the internal stress of a clear acrylic workpiece during ultrasonic vibration-assisted cutting. The following results were obtained.

(1) By activating a 15-ns pulsed laser source in phase with the vibration of the tool, it was possible to visualize the stress fluctuations occurring over extremely short time periods. A constructed photographic system divided the ultrasonic vibration period of 36.2 μs into 360 points and took one photograph frame at each point by combining stroboscopic method. It is experimentally confirmed that the imaging system is able to capture the periodic change of stress distribution in ultrasonic frequency band. The experimental results were agreement with well-known vibration cutting theories.

(2) Observations of the fluctuations in the number of pixels needed to show a specific stress range during vibratory displacement of the tool indicated that the stress range reached a maximum value before the tool reached its forwardmost position. Also, when the depth of cut was shallow, there was a region of the ultrasonic vibratory cycle in which the stress fell to zero. This result demonstrated the intermittent cutting condition. However, once the depth of cut exceeded a set value, stress fluctuations occurred, and the stress no longer fell to zero. It was found that the critical feed speed was influenced by the depth of cut.

(3) The 15-ns pulsed laser realized to capture the propagation of elastic wave. However, no impulsive fluctuations in stress were observed at the moment the ultrasonically vibrating tool struck uncut material.

(4) Remnants formed due to elastic deformation of the workpiece were examined for cutting forces by using a method based on photoelasticity, and the remnant thickness was found to be reduced from 22 μm to a few μm or less by ultrasonic vibration cutting. However, the cutting condition did not become intermittent cutting when the vibration amplitude was 3 μm, because the remnant thickness exceeded that amplitude. But, the remnant thickness was only about 2 μm when the vibration amplitude was 6 μm. It was shown that an amplitude of 6 μm can result in intermittent cutting. These results mean that in order to get the effect of ultrasonic vibration cutting with high production efficiency, remaining uncut should be reduced.

Acknowledgements

We acknowledge Photoron Co.,Ltd for their experimental support. This work was supported by Grant-in-Aid for Scientific Research (B)26289014.

References

[1] Gao F, Zhao B, Jiao F, Liu C. Research on the characteristics of the cutting force in the vibration cutting of a particle-reinforced metal matrix composites SiCp/Al. J Mater Process Technol 2002;129(1–3):196–9.
[2] Mumhammad R, Maurotto A, Roy A, Silberschmidt V. Hot ultrasonically assisted turning of β-Ti alloy. Procedia CIRP 2012;1:336–41.
[3] Hara K, Isobe H. Effect of cutting speed on ultrasonically added turning in soft magnetic stainless steel. Adv Mater Res 2015;806:390–3.
[4] Yamazaki T, Tsuchiya K, Sato U. Ultrasonic vibration cutting of Ti-6mass%Ai-4mass%V alloy. J Jpn Inst Light Metals 2007;57(4):152–6 (in Japanese).
[5] Isobe H, Uehara Y, Kara K, Mihara A. Experimental verification of machining process of ultrasonic drilling. Key Eng Mater 2012;516:275–80.
[6] Isobe H, Kazuya K, Hara K. Improvement of cutting performance by ultrasonic vibration drilling. J Jpn Soc Abras Technol 2015;59(6):328–33 (in Japanese).
[7] Wang J, Zha H, Feng P, Jianfu Zhang J. On the mechanism of edge chipping reduction in rotary ultrasonicdrilling. A novel experimental method. Precis Eng 2016;44:231–5.
[8] Egashira K, Kumagai R, Okina R, Yamaguchi K, Ota M. Drilling of microholes down to 10um in diameter using ultrasonicgrinding. Precis Eng 2014;38(3):605–10.
[9] Lv D, Wang H, Tang Y, Huang Y, Li Z. Influences of vibration on surface formation in rotary ultrasonic machining of glass BK7. Precis Eng 2013;37:839–48.
[10] Wang Y, Suzuki N, Shamoto E, Zhao Q. Investigation of tool wear suppression in ultraprecision diamond machining of die steel. Precis Eng 2011;35:677–85.

[11] Saito H, Jung H, Shamoto E. Elliptical vibration cutting of hardened die steel with coated carbide tools. Precis Eng 2016. PRE-633 P.11 (in press).
[12] Isobe H, Yamaguchi C. High-speed capturing of stress distribution of workpiece under ultrasonically assisted cutting condition. J Jpn Soc Precis Eng 2015;81(5):441–5 (in Japanese).
[13] Onuma T, Otani YA. Dynamic measurement system for two-dimensional birefringence distribution with sub-millisecond time resolution. J Jpn Soc Precis Eng 2012;78(12):1082–6 (in Japanese).
[14] Umezawa E. Stress distribution measurement techniques using photoelasticity: current status and future prospects. J Jpn Soc Precis Eng 2013;79(7):607–10 (in Japanese).
[15] Kumabe A, Yamamoto K. Study on behavior of cutting strain in ductile material by photoelastic coating method. J Jpn Soc Precis Eng 1988;54(11):2144–8 (in Japanese).
[16] Sasahara H, Harada K. Cutting mechanism on ultrasonic vibration cutting. J Jpn Soc Precis Eng 2004;70(4):578–82 (in Japanese).